PHYSICAL REVIEW D **73,** 114502 (2006)

Unquenched determination of the kaon parameter B_K from improved staggered fermions

Elvira Gámiz,* Sara Collins, and Christine T. H. Davies†
Department of Physics & Astronomy, University of Glasgow, Glasgow, G12 8QQ, UK

G. Peter Lepage
Laboratory of Elementary-Particle Physics, Cornell University, Ithaca, New York 14853, USA

Junko Shigemitsu
Physics Department, The Ohio State University, Columbus, Ohio 43210, USA

Matthew Wingate
Institute for Nuclear Theory, University of Washington, Seattle, Washington 98115, USA

(HPQCD and UKQCD Collaborations)

(Received 28 March 2006; published 9 June 2006)

The use of improved staggered actions (HYP, Asqtad) has been proved to reduce the scaling corrections that affected previous calculations of B_K with unimproved (standard) staggered fermions in the quenched approximation. This improved behavior allows us to perform a reliable calculation of B_K including quark vacuum polarization effects, using the MILC configurations with $n_f = 2 + 1$ flavors of sea fermions. We perform such a calculation for a single lattice spacing, $a = 0.125$ fm, and with kaons made up of degenerate quarks with $m_s/2$. The valence strange quark mass m_s is fixed to its physical value and we use two different values of the light sea quark masses. After a chiral extrapolation of the results to the physical value of the sea quark masses, we find $\hat{B}_K = 0.83 \pm 0.18$, where the error is dominated by the uncertainty in the lattice to continuum matching at $O(\alpha_s^2)$. The matching will need to be improved to get the precision needed to make full use of the experimental data on ε_K to constrain the unitarity triangle.

DOI: 10.1103/PhysRevD.73.114502 PACS numbers: 12.38.Gc, 11.15.Ha

I. INTRODUCTION

In the last few years lattice calculations have started achieving the level of precision and the control of uncertainties necessary to extract phenomenologically relevant results [1]. Simulations that incorporate quark vacuum polarization effects are required for this task, since the uncontrolled errors associated with the quenched approximation are usually the main source of uncertainty in these calculations. An example of this can be seen in the study of indirect CP violation in the neutral kaon system.

The CP violating effects in $K^0 - \overline{K^0}$ mixing are parametrized by ε_K, which is defined in terms of the decay amplitudes of the physical neutral kaon states K_L and K_S into a state of two pions with isospin equal to 0 as

$$\varepsilon_K = \frac{A(K_L \to (\pi\pi)_{I=0})}{A(K_S \to (\pi\pi)_{I=0})}. \tag{1}$$

Experimentally, this quantity is known with a precision of a few percent. On the other hand, the theoretical calculation in the standard model, under reliable assumptions, yields the expression

$$\varepsilon_K \simeq \frac{e^{i\pi/4}}{\sqrt{2}\Delta M_K} \mathrm{Im} M_{12}, \tag{2}$$

where ΔM_K is the mass difference between K_L and K_S, a very well measured quantity, and M_{12} is defined by

$$2m_K M_{12}^* = \langle \overline{K^0} | H_{\mathrm{eff}}^{\Delta S=2} | K^0 \rangle. \tag{3}$$

ε_K is thus determined by the hadronic matrix element between K^0 and $\overline{K^0}$ of the $\Delta S = 2$ effective Hamiltonian

$$H_{\mathrm{eff}}^{\Delta S=2} = C_{\Delta S=2} C(\mu) \int d^4x Q_{\Delta S=2}(x) \tag{4}$$

with

$$Q_{\Delta S=2}(x) = [\bar{s}_a \gamma_\mu d_a]_{V-A}(x) [\bar{s}_b \gamma^\mu d_b]_{V-A}(x). \tag{5}$$

The Wilson coefficient $C(\mu)$ is a perturbative quantity known to NLO in α_s in both the Naive Dimensional Regularization (NDR) and the 't Hooft-Veltman (HV) schemes. The coefficient $C_{\Delta S=2}$ includes known functions of the masses of particles that have been integrated out, and also depends on a certain combination of Cabibbo-Kobayashi-Maskawa (CKM) matrix elements. It is these

*Electronic address: e.gamiz@physics.gla.ac.uk
†Electronic address: c.davies@physics.gla.ac.uk

latter elements about which we would like to obtain information. The combination of CKM parameters entering in $C_{\Delta S=2}$ is $\mathrm{Im}(V_{ts}V_{td}^*)^2$, which is equivalent to the unitarity triangle (UT) combination of parameters $\bar{\eta}[(1-\bar{\rho})+\text{const.}]$ [2]. For reviews where explicit expressions for the coefficients in (4) can be found, see [3]. The two-loop expression for the Wilson coefficient $C(\mu)$ is given by

$$C(\mu)=\left(1+\frac{\alpha_{\overline{MS}}(\mu)}{4\pi}4\left[\frac{\gamma_1}{\beta_0}-\frac{\beta_1\gamma_0}{\beta_0^2}\right]\right)[\alpha_{\overline{MS}}(\mu)]^{\gamma_0/\beta_0}, \tag{6}$$

where γ_0, γ_1 are the $\Delta S=2$ anomalous dimension at one-loop and two-loop, respectively, and β_0, β_1 are the first two coefficients of the QCD beta function. $\gamma_0=1$ is independent of the number of flavors n_f, while the other quantities depend on n_f in the following way

$$\beta_0=-\frac{1}{2}\left(11-\frac{2n_f}{3}\right);\qquad \beta_1=-\frac{1}{8}\left(102-\frac{38n_f}{3}\right);$$
$$\gamma_1^{\overline{MS}-NDR}=\frac{1}{16}\left(-7+\frac{4n_f}{9}\right); \tag{7}$$

where only the NLO coefficient γ_1 depends on the choice of scheme and it is given in the $\overline{MS}(NDR)$ scheme we are going to use to quote the results in this work. The other coefficients are universal. Although $C(\mu)$ depends analytically on the number of flavors through the parameters in (7), the numerical dependency on n_f in the conversion from the $\overline{MS}(NDR)$ scheme value $B_K^{\overline{MS}-NDR}(2\ \mathrm{GeV})$ to $\hat{B}_K$ is negligible [4].

The matrix element $\langle\overline{K^0}|Q_{\Delta S=2}|K^0\rangle$, that encodes the nonperturbative physics of the problem, is usually normalized by its vacuum insertion approximation (VIA) value, defining B_K as the ratio

$$B_K(\mu)\equiv\frac{\langle\overline{K^0}|Q_{\Delta S=2}(\mu)|K^0\rangle}{\frac{8}{3}\langle\overline{K^0}|\bar{s}\gamma_0\gamma_5 d|0\rangle\langle 0|\bar{s}\gamma_0\gamma_5 d|K^0\rangle}. \tag{8}$$

The renormalization group invariant form of B_K, the so-called $\hat{B}_K$, is often used to quote results. It is defined as

$$\hat{B}_K=C(\mu)B_K(\mu), \tag{9}$$

with $C(\mu)$ the Wilson coefficient in the effective Hamiltonian (4), given at two-loops in (6).

One can try to constrain the value of the combination of CKM matrix elements in $C_{\Delta S=2}$ using the experimental value of ε_K and a theoretical calculation of B_K. That constraint gives a hyperbole in the $\rho-\eta$ plane, where ρ and η are the usual UT parameters [2]. The largest source of uncertainty in the final results comes from the error in the determination of B_K [5,6]. Improvement in the calculation of this kaon parameter, to reach at least the same level of precision (a few percent) as the rest of the errors entering in the analysis of ε_K, is thus crucial in order to get information about the UT. In addition, ε_K can be a very powerful probe of new physics [7].

Because of the phenomenological relevance of B_K its calculation has been addressed many times using different techniques. The three main continuum QCD-based approaches that have been used in its determination are QCD-Hadron duality [8], three-point function QCD sum rules [9] and the $1/N_c$ ($N_c=$ number of colors) expansion [10,11]. Many of these determinations give results for B_K only in the chiral limit, since that is a very well established limit in the continuum that simplifies the calculation considerably. Chiral corrections however are essential to get a value of B_K useful for phenomenologists, since they represent more than 50% of the final number [11]. In fact there is only one recent determination of the physical B_K [11], although there is work in progress to calculate chiral corrections to this parameter in the framework of the $1/N_c$ expansion [12,13].

The fourth technique that has been used to calculate B_K is lattice gauge theory. It offers model independent results and has the potential to reduce the error to the level required by phenomenology. Reviews of lattice determinations of B_K in the quenched approximation and some preliminary results including quark vacuum polarization effects can be found in [14].

So far, the value of B_K that the phenomenologists have been using in their studies of the UT [5] is a lattice result by the JLQCD collaboration [15] which uses unimproved staggered quarks in the quenched approximation. That is the most complete analysis of B_K with lattice techniques to date. The value given in [15] is $B_K^{\overline{MS}-NDR}(2\ \mathrm{GeV})=0.628\pm0.042$, which corresponds to $\hat{B}_K=0.86\pm0.06$. This number is the result from the extrapolation to the continuum limit of the values obtained for seven lattice spacings, with both gauge invariant and noninvariant operators—see Sec. II C—and the error includes an estimate of order α^2 and a^2 corrections. Finite volume effects were also studied for two different values of a.

The main source of uncertainty in the JLQCD calculation (not included in the quoted uncertainty) is the unknown error from quenching, which could be as large as 15% according to the chiral perturbation theory (CHPT) estimate performed in [16]. In order to have a prediction at a few percent level it is thus necessary to perform unquenched calculations of B_K that eliminate the quenching uncertainties. Such calculations have now become feasible.

Another feature of the calculation in [15] is that it is affected by large scaling violations. We will see that the scaling behavior is much better using improved staggered actions instead of the standard unimproved staggered action used by the JLQCD collaboration.

A third way of improving the JLQCD calculation would be to incorporate SU(3) breaking effects by using kaons made up of nondegenerate quarks, instead of degenerate quarks with $m_s/2$. However, these effects are not expected

to be important as first estimated using CHPT by Sharpe [16] (the effects were estimated to be $\sim 5\%$) and as the preliminary results from unquenched domain wall [17] and staggered [18] quarks seem to indicate (the authors found differences $\sim 3\%$ between the degenerate and nondegenerate results).

The goal of this work is to perform a calculation of B_K including quark vacuum polarization effects, which will eliminate the irreducible and unknown quenching uncertainty. In this calculation we will use improved staggered fermions that have been proved to reduce the large $\mathcal{O}(a^2)$ discretization errors generated by the taste-changing interactions.

Preliminary results from this study were presented in [19]. The matching coefficients needed in the calculation of the renormalized B_K with the action used in our unquenched simulations were not available at that time, so an approximate renormalization was performed in order to get those preliminary results. The correct renormalization coefficients have since been calculated [20] and have been used to obtain the results reported in [21] and in the present article—see next section for more details about the renormalization process.

Other recent preliminary unquenched results can be found in [17,18,22–25].

II. THEORETICAL FRAMEWORK

In this section we briefly describe the fermion formalism we are going to use in this work, the staggered formalism, as well as the fermion and gauge actions used in the quenched and unquenched calculations reported here. We also set up the notation for the lattice operators needed in our study and justify our choice of external states.

A. Staggered fermions

When the quark action is written in terms of staggered fermions, it becomes spin diagonal and we can drop three of the four components of the staggered field χ. The standard (unimproved) form of the staggered fermion action is thus

$$\mathcal{S}_f^{\text{unim}} = \sum_n \Big[\frac{1}{2} \sum_\mu \eta_\mu(n) (\bar{\chi}(n) U_\mu(n) \chi(n+\hat{\mu}) - \bar{\chi}(n+\hat{\mu}) U_\mu^\dagger(n) \chi(n)) + m \bar{\chi}(n) \chi(n) \Big], \quad (10)$$

where $n = (n_1, n_2, n_3, n_4)$ parametrizes the lattice site, $\eta_\mu(n) = (-1)^{n_1 + \cdots + n_{\mu-1}}$ and χ is a 3(colors) $\times$ 1(spin) component object. The relation between the staggered field χ and the naive fermion field Ψ at each lattice site is

$$\Psi(n) = \Gamma_n \chi(n) \qquad \bar{\Psi}(n) = \bar{\chi}(n) \Gamma_n^\dagger, \quad (11)$$

with

$$\Gamma_n = (\gamma_1)^{n_1} (\gamma_2)^{n_2} (\gamma_3)^{n_3} (\gamma_4)^{n_4}. \quad (12)$$

The staggered action has a remnant of chiral symmetry which ensures that the Goldstone boson pion mass vanishes at $ma = 0$. But the main advantage of staggered fermions is that they are computationally very efficient and unquenched simulations with three flavors of sea quarks are possible at present with lighter sea quark masses than those achieved with other fermion formulations.

The fundamental disadvantage suffered by staggered fermions is the fact that each flavor field comes in four different tastes. In the continuum limit the four tastes are degenerate and extra copies can be removed by hand. For sea quarks this involves taking the fourth-root of the quark determinant in unquenched simulations and, in perturbation theory, the division of each fermion loop by a factor of 4. The validity of the fourth root procedure has not been rigorously proven but tests of it are encouraging [26]. At nonzero lattice spacing the situation is more complicated due to the existence of interactions of $\mathcal{O}(a^2)$ that violate the taste symmetry and are potentially dangerous. However, the negative effects of these taste-changing interactions can be reduced by adding improvement terms to the action as pointed out in [27]. This issue is discussed in more detail in the following section.

B. Improved staggered actions

Large $\mathcal{O}(a^2)$ discretization errors have been found in the calculation of masses and matrix elements using unimproved staggered fermions. The origin of these anomalously large discretization errors, as well as other effects, such as the large size of perturbative corrections, are the taste-changing interactions that break the taste symmetry at nonzero lattice spacing. These (unphysical) interactions can be systematically removed using the method of Symanzik and replacing the gauge link U in (10) by a fat link V, that is a weighted combination of different staples. For studies of the effects of using fat links see [28–30].

In the quenched simulations in Sec. IV, we use two different improved actions, the HYP and the Asqtad. The construction of the HYP [31] action involves three levels of APE smearing with projection onto SU(3) at each level. The smearing is restricted in such a way that each fat link includes contributions only from thin links belonging to hypercubes attached to the original link.

The Asqtad action we analyze here and use in our unquenched simulations has been extensively used in the past for simulating light sea and valence quarks [32]. It has been designed to reduce the taste symmetry breaking effects and remove all other $\mathcal{O}(a^2)$ discretization errors. The virtue of this improved action is that it allows for precise calculations with light sea quarks.

Together with the fat links, the other ingredients that differentiate the fermion part of the Asqtad action from the unimproved one are the so-called Lepage corrections and the Naik term. The Asqtad action, written in terms of four component *naive* fermions, has the form

$$\mathcal{S}_f^{\text{Asqtad}} = a^4 \sum_x \left\{ \bar{\Psi}(x) \left[\sum_\mu \gamma_\mu \frac{1}{a} \left(\nabla'_\mu - \frac{1}{6} \nabla_\mu^{3-\text{link}} \right) + m \right] \Psi(x) \right\}, \tag{13}$$

with

$$\begin{aligned} \nabla_\mu^{3-\text{link}} \Psi(x) &= (\nabla_\mu)^3 |_{\text{tadpole improved}} \Psi(x) \\ &= \frac{1}{8} \left\{ \frac{1}{u_0^3} [UUU\Psi(x + 3a_\mu) \right. \\ &\quad - U^\dagger U^\dagger U^\dagger \Psi(x - 3a_\mu)] \\ &\quad \left. - \frac{3}{u_0} [U\Psi(x + a_\mu) - U^\dagger \Psi(x - a_\mu)] \right\}, \end{aligned} \tag{14}$$

and ∇'_μ being the usual covariant derivative with the thin link variable U_μ replaced by an updated variable $V'_\mu(x) \equiv V_\mu(x) - \sum_{\rho \neq \mu} \frac{(\nabla_\rho^\ell)^2}{4} U_\mu(x)$. In this expression $V_\mu(x)$ is the fat link

$$V_\mu(x) \equiv \prod_{\rho \neq \mu} \left(1 + \frac{\nabla_\nu^{\ell,(2)}}{4} \right) \Big|_{\text{symmetrized}} U_\mu(x) \tag{15}$$

and the second term is the Lepage term that removes a low momentum $\mathcal{O}(a^2)$ error. For the exact definitions of the derivatives ∇_ν^ℓ and $\nabla_\nu^{\ell,(2)}$ see, for example, [33].

The Asqtad fermion action is coupled in the unquenched simulations to an SU(3) gluonic action that is one-loop Symanzik improved after tadpole improvement [34,35]. In the quenched calculations, instead of using the improved gluon action, we use the usual unimproved Wilson glue action.

C. Definition of the operators

To construct the four-fermion operators, we collect the staggered fields χ into a set of Dirac fields $q(2N)$ that live on the even lattice sites and are spread over a unit hypercube [36]

$$q(2N)_{\alpha,i} = \frac{1}{8} \sum_A (\Gamma_A)_{\alpha,i} \chi(2N + A), \tag{16}$$

where α and i are the Dirac and taste indices, respectively, and with A running over the vertices of a hypercube ($A_\mu = 0$ or 1, $\mu = 1, \ldots, 4$). The bilinear quark operators with spin structure $\gamma_S = \Gamma_S$ and taste structure $\xi_T = \Gamma_T^*$ are defined by

$$\begin{aligned} \mathcal{O}_{\mathcal{ST}} &= \bar{q}(2N)(\gamma_S \otimes \xi_T) q(2N) \\ &= \frac{1}{16} \sum_{A,B} \bar{\chi}(2N + A) \chi(2N + B) \frac{1}{4} \text{tr}(\Gamma_A^\dagger \gamma_S \Gamma_B \Gamma_T^\dagger) \end{aligned} \tag{17}$$

The four-quark operators can be built with the bilinears in (17) considering two different contractions of the color indices

$$\begin{aligned} \mathcal{O}_1 &= \bar{q}^a (\gamma_{S_1} \otimes \xi_{T_1}) q^b \cdot \bar{q}^b (\gamma_{S_2} \otimes \xi_{T_2}) q^a \\ &= \left(\frac{1}{16} \right)^2 \sum_{ABCD} \bar{\chi}_A^a \frac{1}{4} \text{tr}(\Gamma_A^\dagger \gamma_{S_1} \Gamma_B \Gamma_{T_1}^\dagger) \chi_B^b \\ &\quad \cdot \bar{\chi}_C^b \frac{1}{4} \text{tr}(\Gamma_C^\dagger \gamma_{S_2} \Gamma_D \Gamma_{T_2}^\dagger) \chi_D^a, \\ \mathcal{O}_2 &= \bar{q}^a (\gamma_{S_1} \otimes \xi_{T_1}) q^a \cdot \bar{q}^b (\gamma_{S_2} \otimes \xi_{T_2}) q^b \\ &= \left(\frac{1}{16} \right)^2 \sum_{ABCD} \bar{\chi}_A^a \frac{1}{4} \text{tr}(\Gamma_A^\dagger \gamma_{S_1} \Gamma_B \Gamma_{T_1}^\dagger) \chi_B^a \\ &\quad \cdot \bar{\chi}_C^b \frac{1}{4} \text{tr}(\Gamma_C^\dagger \gamma_{S_2} \Gamma_D \Gamma_{T_2}^\dagger) \chi_D^b, \end{aligned} \tag{18}$$

where we have suppressed the hypercube label $2N$ for simplicity. The operators in (18) are known as one-color-trace and two- color-trace operators, respectively.

To make these operators gauge invariant we insert gauge link factors connecting the quark fields according to

$$\begin{aligned} \mathcal{O}_1 &= \left(\frac{1}{16} \right)^2 \sum_{ABCD} \bar{\chi}_A^{a n_{f_1}} \frac{1}{4} \text{tr}(\Gamma_A^\dagger \gamma_{S_1} \Gamma_B \Gamma_{T_1}^\dagger) \chi_B^{b n_{f_2}} \\ &\quad \cdot \bar{\chi}_C^{c n_{f_3}} \frac{1}{4} \text{tr}(\Gamma_C^\dagger \gamma_{S_2} \Gamma_D \Gamma_{T_2}^\dagger) \chi_D^{d n_{f_4}} \cdot U_{AD}^{ad} U_{CB}^{cb}, \\ \mathcal{O}_2 &= \left(\frac{1}{16} \right)^2 \sum_{ABCD} \bar{\chi}_A^{a n_{f_1}} \frac{1}{4} \text{tr}(\Gamma_A^\dagger \gamma_{S_1} \Gamma_B \Gamma_{T_1}^\dagger) \chi_B^{b n_{f_2}} \\ &\quad \cdot \bar{\chi}_C^{c n_{f_3}} \frac{1}{4} \text{tr}(\Gamma_C^\dagger \gamma_{S_2} \Gamma_D \Gamma_{T_2}^\dagger) \chi_D^{d n_{f_4}} \cdot U_{AB}^{ab} U_{CD}^{cd}. \end{aligned} \tag{19}$$

Here, we suppress again the hypercube label $2N$ for simplicity and add superscripts n_{f_i} to label the different continuum flavors. Notice that we consider fat links only in the action and those that we introduce in the operators are thin links. The only improvement in the operators we consider is tadpole improvement. This we carry out by dividing the gluon fields by appropriate factors of the mean link u_0 defined as the fourth root of the average plaquette. The operators used in the calculation with improved actions are thus exactly the same as those used in the unimproved simulations. In this work we also use gauge noninvariant operators, that do not incorporate gauge link factors but instead are calculated on gluon configurations fixed to Landau gauge.

In the transcription of the continuum operators involved in the calculation of B_K to the staggered ones we have to take into account the taste degree of freedom. We choose the external kaon to have taste structure $\xi_T = \gamma_5$ (and thus fix the taste structure of the vector and axial operators with nonzero matrix elements), since only the mesons with such structure become massless in the chiral limit. In addition, in order to avoid mixing with operators with different taste structure, we follow the two-spin-trace formalism described in Refs. [37,38] and introduce two sets of valence

quarks s_1, d_1 and s_2, d_2 for each of the bilinears constituting the four-fermion operator $Q_{\Delta S=2}$. Matrix elements are then taken between kaons $K_1^0 = \bar{s}_1 d_1$ and $\overline{K_2^0} = \bar{d}_2 s_2$. A detailed explanation of the two-spin-trace formalism for B_K can be found in [37,38].

III. PERTURBATIVE RENORMALIZATION

An important step needed in the determination of B_K (as well as any renormalized quantity) is the calculation of the coefficients that match the lattice matrix elements to the continuum ones. The operator $Q_{\Delta S=2}$ in (4) is renormalized multiplicatively if one has a regularization with exact chiral symmetry, such as the dimensional regularization in the continuum or Ginsparg-Wilson fermions on the lattice. For staggered fermions, although full chiral symmetry is broken at nonzero lattice spacing, there is a remnant $U(1)$ symmetry which allows us to have the mixing under control at a given order in perturbation theory. In particular, the one-loop calculation involves only four operators, as explained below.

In this work we use a one-loop perturbative matching to relate the lattice and continuum operators. A general one-loop matching of the bare lattice operators O_j^{latt} to the renormalized continuum operators O_i^{cont} at an intermediate scale μ can be expressed as

$$O_i^{\text{cont}}(\mu) = O_i^{\text{latt}} + \frac{\alpha_s(q^*)}{4\pi}\sum_j (-\gamma_1^{ij}\ln(\mu a) + C_{ij})O_j^{\text{latt}} + \mathcal{O}(\alpha_s(q^*)^2), \tag{20}$$

with γ_1^{ij} the one-loop anomalous dimensions matrix and C_{ij} the one-loop matching coefficients, depending on the continuum scheme.

The operator $Q_{\Delta S=2}$ is the product of two $V-A$ currents. The QCD corrections to the bare lattice four-quark operators affect the vector and axial parts differently; as a consequence currents of the form $V+A$ are generated. A minimal set of lattice operators that matches to the continuum, closes under renormalization and has nonvanishing $K-\bar{K}$ matrix elements is

$$\begin{aligned} V^{(1)} &= (\bar{s}^a d^b)_V (\bar{s}^b d^a)_V, & V^{(2)} &= (\bar{s}^a d^a)_V (\bar{s}^b d^b)_V, \\ A^{(1)} &= (\bar{s}^a d^b)_A (\bar{s}^b d^a)_A, & A^{(2)} &= (\bar{s}^a d^a)_A (\bar{s}^b d^b)_A, \end{aligned} \tag{21}$$

where V and A are the vector and axial currents with taste structure $\xi_T = \gamma_5$. The color indices a, b indicate which fields are connected by gauge link factors, according to (19). The superscripts 1 and 2 indicate that they are one-color-trace or two- color-trace operators.

Perturbative calculations and nonperturbative simulations have to be done with exactly the same action and operators. The one-loop lattice to continuum matching coefficients for the $\Delta S = 2$ four-quark operators in (21) have been calculated for unimproved staggered fermions [39], as well as for HYP staggered fermions [40]; although this last calculation only considered gauge invariant operators. The matching calculation for the Asqtad action, with both a Wilson gauge action and an improved gauge action as described in Sec. II B, was done perturbatively at one-loop in [20] for gauge invariant as well as gauge non-invariant operators for a general gauge.

The calculation in [20] was performed with two independent methods. First, the authors evaluated the corresponding one-loop diagrams in two different ways: by directly calculating the various diagrams and by first separating off the part which can be inferred from the renormalization of the current operators. Second, the lattice integrals were evaluated both algebraically and numerically. For the algebraic evaluation, the authors in [20] expanded the diagrams around the continuum limit. This produces a set of lattice tadpole integrals which one then reduces to a minimal set of master integrals using computer algebra. The agreement between these two rather different methods provides a strong check on their results.

The size of the one-loop corrections to the tree level matching for the Asqtad action (with and without improved glue) is very similar to what is found with unimproved staggered and other improved staggered actions, such as the HYP action. In the calculation of B_K thus the reason to use an improved action is not the reduction of the matching factors (which are not large in the unimproved calculation) but the correction of the bad scaling behavior, as we have already pointed out. That is not the case with other weak matrix elements relevant in the study of CP-violating effects, for which the use of improved staggered actions greatly reduces the size of the perturbative matching coefficients—see [20] for further discussions and references.

Two comments are in order with respect to the results in [20]. First, the authors found that the matching coefficients obtained for the Asqtad action with improved glue are very similar to those with an unimproved glue action—see Eqs. (22) and (23) below. They conclude that the improvement in the glue action is not crucial in order to reduce the size of the perturbative coefficients, as already suggested in [41]. Another conclusion from that work is that we do not expect anomalously large $\mathcal{O}(\alpha_s^2)$ corrections using the Asqtad action.

For completeness, we write here the matrices C_{ij} in (20), taken from [20], that must be used to obtain $\langle\overline{K^0}|Q_{\Delta S=2}(\mu)|K^0\rangle^{\overline{MS}}$ from the Asqtad bare matrix elements in the appendix. They are written in the basis $(V^{(1)}, V^{(2)}, A^{(1)}, A^{(2)})$. They are

$$C_{\text{inv}}^{\text{unimp. glue}} = \begin{pmatrix} -14.3796 & 1.3606 & -0.0520 & -0.0394 \\ 3 & -19.8263 & -0.0389 & 0.0263 \\ -0.0520 & -0.0394 & -15.1796 & 3.8005 \\ -0.0389 & 0.0263 & 3 & -10.6495 \end{pmatrix},$$
$$C_{\text{noninv}}^{\text{unimp. glue}} = \begin{pmatrix} -12.3228 & 2.6405 & -0.0520 & -0.0394 \\ 3 & -13.4411 & -0.0389 & 0.0263 \\ -0.0520 & -0.0394 & -12.4428 & 3.0005 \\ -0.0389 & 0.0263 & 3 & -12.4811 \end{pmatrix}, \tag{22}$$

for both gauge invariant and gauge noninvariant operators (in the Landau gauge) using an unimproved glue action. And

$$C_{\text{inv}}^{\text{imp. glue}} = \begin{pmatrix} -15.1091 & 1.7606 & 0.5080 & 0.2406 \\ 3 & -19.3177 & 0.4411 & -0.1337 \\ 0.5080 & 0.2406 & -15.8691 & 4.0806 \\ 0.4411 & -0.1337 & 3 & -10.8972 \end{pmatrix},$$
$$C_{\text{noninv}}^{\text{imp. glue}} = \begin{pmatrix} -12.0486 & 2.9206 & 0.05080 & 0.2406 \\ 3 & -12.2869 & 0.4411 & -0.13370 \\ 0.5080 & 0.2406 & -12.1687 & 3.2806 \\ 0.4411 & -0.1337 & 3 & -11.3269 \end{pmatrix}, \tag{23}$$

for gauge invariant operators and gauge noninvariant operators using the improved gluon action. These results are obtained after tadpole improvement with the mean link u_0 defined as the fourth root of the average plaquette. The one-loop contribution to this parameter is $u_0^{(1)} = \pi/3$ for the unimproved gluon action and $u_0^{(1)} = 0.7671$ for the improved gluon action, where $u_0^{(1)}$ is defined as $u_0 = 1 - \alpha_s u_0^{(1)} + \mathcal{O}(\alpha_s^2)$.

In addition to the matching for the four-fermion matrix element in (8) we must also account for the renormalization of the axial currents in the denominator of (8), which is nonvanishing with the Asqtad action for the definition of the axial current of (21). The axial current renormalization is multiplicative and can be written in the form $1 + \alpha_s/\pi Z_A$, with $Z_{A,\text{unimp}}^{\text{inv}} = 1.206$, $Z_{A,\text{imp}}^{\text{inv}} = 1.237$ when using unimproved and improved glue, respectively, with gauge invariant operators, and $Z_{A,\text{unimp}}^{\text{noninv}} = 1.435$, $Z_{A,\text{imp}}^{\text{noninv}} = 1.291$ when using unimproved and improved glue with gauge noninvariant operators in the Landau gauge.

IV. SCALING BEHAVIOR OF THE IMPROVED STAGGERED ACTIONS

The first issue we analyze is the impact of using improved staggered actions in the calculation of B_K, in comparison with the unimproved staggered action analyzed in [15]. This study is carried out in the quenched approximation and for two different improved actions: the HYP [31] and the Asqtad with Wilson glue.

In the next two subsections we describe the results obtained for gauge invariant operators only. We postpone the discussion on the differences found between using gauge invariant and gauge noninvariant operators until the last subsection IV C.

A. Simulation details

We have two ensembles of 150 and 50 configurations at $\beta = 5.70$ and $\beta = 5.93$ respectively, generated using the Wilson gluon action for the three staggered fermion actions that we are going to analyze, unimproved, HYP and Asqtad. The values of the parameters used in the simulations are shown in Table I. We choose these parameters to be the same as those used by the JLQCD collaboration in order to make a clear comparison with their results. In particular, we match kaon masses at a given β to those of the JLQCD collaboration [42], which fixes the strange quark mass to the values listed in Table I. The lattice spacings, determined from m_ρ, are also taken from Ref. [42], again for consistent comparison with that work. For the same reason, we consider kaons made up with two degenerate quarks of $m_s/2$ as in [42].

Within the conventions and parameters we have described above, the bare values of B_K we obtain are plotted in Fig. 1 as a function of the time slice for the three actions and for the two different values of the lattice spacing. The $\beta = 5.70$ and $\beta = 5.93$ results present a plateau for $3 \leq t \leq 10$ and $5 \leq t \leq 12$ respectively, so we make fits to a constant over those ranges of values of t. The results from those fits are also plotted in Fig. 1 and the numerical values

TABLE I. Parameters in the quenched simulations. The values for $m_s/2$ are for the HYP and Asqtad staggered actions, respectively.

β	Volume	n_{confs}	a^{-1} (GeV)	$am_s/2$	La (fm)	am_K	$\alpha_s(1/a)$
UKQCD $n_f = 0$							
5.7	$12^3 \times 24$	150	0.837(6)	0.086/0.064	2.9	0.417	0.31
5.93	$16^3 \times 32$	50	1.59(3)	0.039/0.030	2.0	0.220	0.21

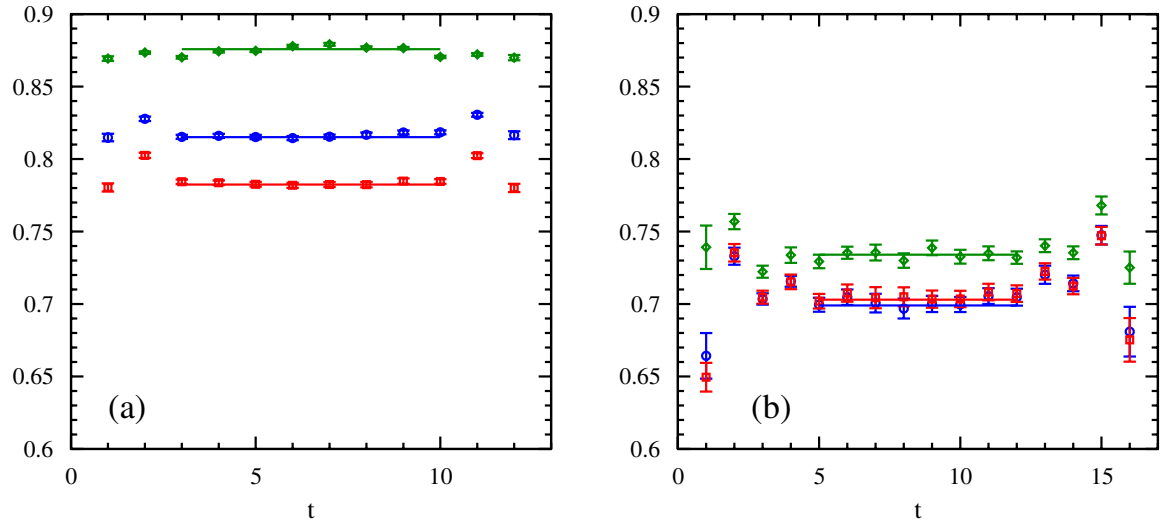

FIG. 1 (color online). Values of the bare gauge invariant B_K at $\beta = 5.70$ (a) and 5.93 (b) for unimproved (green diamonds), HYP (red squares) and Asqtad (blue circles) quarks. Solid lines show results from our fits.

summarized in Table II. Individual values for the four four-fermion bare lattice operators in (21) normalized to the bare lattice value of the numerator in (8) are given in Tables V, VI, and VII in the appendix.

TABLE II. Bare B_K and renormalized $B_K^{\overline{MS}-NDR}(2\text{ GeV})$ for both gauge invariant and noninvariant operators in the quenched approximation using unimproved, Asqtad and HYP staggered fermions. The errors quoted in this table are only statistical.

$B_K^{\text{bare}}(n_f = 0)$		
β	invariant	noninvariant
	$n_f = 0$ unimproved	
5.7	0.876(1)	0.895(1)
5.93	0.734(5)	0.722(3)
	$n_f = 0$ Asqtad	
5.7	0.815(1)	0.824(1)
5.93	0.699(7)	0.708(4)
	$n_f = 0$ HYP	
5.7	0.782(1)	-
5.93	0.703(5)	-

$B_K^{\overline{MS}-NDR}(2\text{ GeV})(n_f = 0)$		
β	invariant	noninvariant
	$n_f = 0$ unimproved	
5.7	0.816(1)	0.841(1)
5.93	0.720(3)	0.747(3)
	$n_f = 0$ Asqtad	
5.7	0.715(1)	0.729(1)
5.93	0.647(4)	0.673(4)
	$n_f = 0$ HYP	
5.7	0.648(1)	-
5.93	0.627(4)	-

B. Results

To convert the lattice results to the $\overline{MS} - NDR$ scheme we use the one-loop coefficients from [20,39,40] as appropriate, with the matching scale μ and the scale for α_s equal to $\mu = q^* = 1/a$. The values for the coupling constant $\alpha_s(q^* = 1/a)$ used in the matching process for the different lattice spacings, are again taken from [15] to provide comparison with that work. They use $\alpha_{\overline{MS}-NDR}(1/a)$ as given by $\Lambda_{\overline{MS}} = 230$ MeV. Their values are listed in Table I. After this process we obtain the renormalized continuum value $B_K^{\overline{MS}-NDR}(1/a)$, that we can run to 2 GeV using the two-loop running of the continuum renormalization group

$$B_K(\mu_1) = \frac{C(\mu_2)}{C(\mu_1)} B_K(\mu_2), \tag{24}$$

where $C(\mu)$ is the Wilson coefficient given in (6) with $n_f = 0$. The renormalization group invariant form $\hat{B}_K$ can be similarly calculated using (6) and its definition in (9).

The results we obtain for $B_K^{\overline{MS}-NDR}(2\text{ GeV})$ for the different actions and the two lattice spacings are given in Table II. In the unimproved case the numbers for gauge invariant and noninvariant operators agree well with those of the JLQCD collaboration [15] for both lattice spacings. The quenched results for gauge invariant operators in Table II are plotted as a function of the lattice spacing in Fig. 2. In this figure a clear improvement in the scaling can be seen when using improved actions, in particular, in the HYP case. We can quantify the improvement in the scaling by extrapolating our results for $\beta = 5.70$ and $\beta = 5.93$ to the continuum limit, assuming a quadratic dependence on the lattice spacing. In the unimproved case, the result from this exercise, 0.682, is incompatible with the JLQCD result 0.628, that incorporates an estimate of $\mathcal{O}(a^2)$ and $\mathcal{O}(\alpha_s^2)$

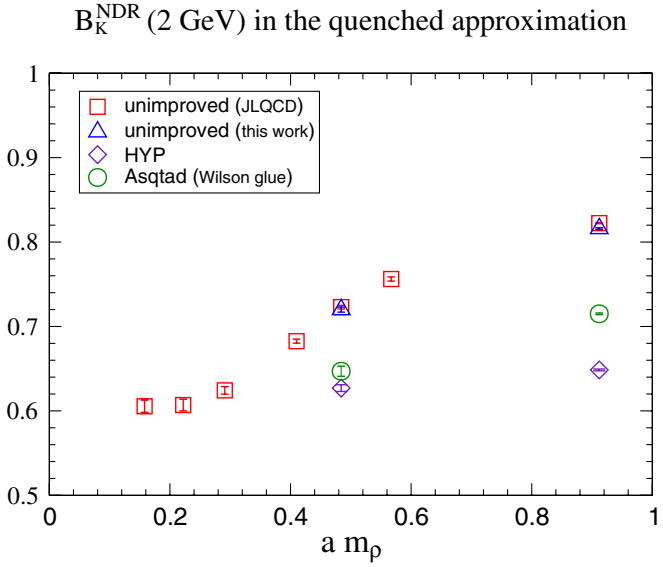

FIG. 2 (color online). Scaling of $B_K^{\overline{MS}-NDR}(2\ \mathrm{GeV})$ with a for improved staggered actions compared to the JLQCD unimproved staggered results. Results in this figure are obtained with gauge invariant operators.

corrections. In fact, in the work by the JLQCD collaboration [15] the authors disregarded the points at $\beta = 5.70$ and $\beta = 5.85$ to perform the extrapolation to the continuum limit since these points did not exhibit the quadratic dependence in a. However, extrapolations of the HYP and Asqtad actions for our two lattice spacings give 0.619 and 0.620 for $B_K^{\overline{MS}-NDR}(2\ \mathrm{GeV})$ in the continuum limit, consistent with the JLQCD result in the continuum limit. We expect such improved scaling to survive unquenching and this therefore allows us to perform reliable unquenched calculations with only a few values of the lattice spacing and even obtain valuable information from simulations at a single scale.

The reduction of the discretization errors for staggered fermions using improved actions has already been shown for other quantities such as hadron masses [29]. In the calculation of B_K it has been recently studied in [43] with the HYP action, leading to the same conclusions as in the present article.

C. Differences between gauge invariant and gauge noninvariant operators results

The final error quoted by the JLQCD collaboration in its unimproved staggered study of B_K [15] was very much enhanced by the differences found between the results obtained with gauge invariant and gauge noninvariant operators. These differences have their origin in $\mathcal{O}(\alpha_s^2)$ and $\mathcal{O}(a^2)$ corrections, which were fitted in [15] leading to uncertainties of the same size as $3\alpha_s^2$ with $\alpha_s = \alpha_{\overline{MS}}(1/a)$.

We have studied this issue with the unimproved as well as with the Asqtad action. A similar analysis with the HYP action is not possible since renormalization coefficients for gauge noninvariant operators in the Landau gauge are not available. The results for the bare B_K as well as the renormalized $B_K^{\overline{MS}-NDR}(2\ \mathrm{GeV})$ obtained with the gauge noninvariant operators defined in Sec. II C are given in Table II. Despite the large improvement in the scaling found for the Asqtad action, the differences between gauge invariant and noninvariant results are of the same size as those observed in the unimproved case. That indicates that these differences are dominated not by the $\mathcal{O}(a^2)$ corrections but by the $\mathcal{O}(\alpha_s^2)$ corrections, as was already pointed out in Ref. [15]. Since the improvement of the action does not lead to a reduction of the perturbative coefficients in the particular case of the calculation of B_K, the differences between the results using the two definitions of operators are not reduced by using the improved actions. It would be necessary to perform a two-loop matching to reduce the uncertainty associated with the definition of the operators.

Another conclusion from the comparison of the Asqtad results in Table II is that those corresponding to gauge invariant operators give values more similar to the JLQCD results as $a \to 0$, which indicates that the $\mathcal{O}(\alpha_s^2)$ corrections are smaller for these operators. We expect thus more accurate results from gauge invariant operators, which is what we use in our unquenched calculation, than from the noninvariant ones.

V. UNQUENCHED VALUE OF B_K

We now incorporate quark vacuum polarization effects in the calculation of B_K using one of the improved staggered actions analyzed in the quenched approximation, Asqtad, since the final goal is to eliminate the irreducible systematic error associated with quenching that dominates the total uncertainty in previous determinations of B_K. We use the Asqtad action because there are configurations for this action generated with sea masses sufficiently small to perform a realistic chiral extrapolation to the physical point [44,45]. In addition, unquenched simulations using this action have been successful in describing a wide range of experimental observables with systematic errors of 3% or less [1].

We performed an unquenched calculation of B_K with the Asqtad action described in Sec. II B, using the configurations from the MILC collaboration with $n_f = 2 + 1$ sea flavors [34]. The results reported here correspond to the analysis at one lattice spacing with $a = 0.125$ fm and two

TABLE III. Parameters in the unquenched simulations. The configurations are taken from the MILC collaboration [34]. The lattice spacings are taken from [46]. Quarks masses are given in the MILC convention, which includes a factor of u_0 compared to the standard convention.

β	n_{confs}	Volume	a^{-1} (GeV)	am_{sea}	$am_s/2$	$\alpha_V(1/a)$
6.76	560	$20^3 \times 64$	1.605	0.01/0.05	0.02	0.47
6.79	414	$20^3 \times 64$	1.596	0.02/0.05	0.02	0.47

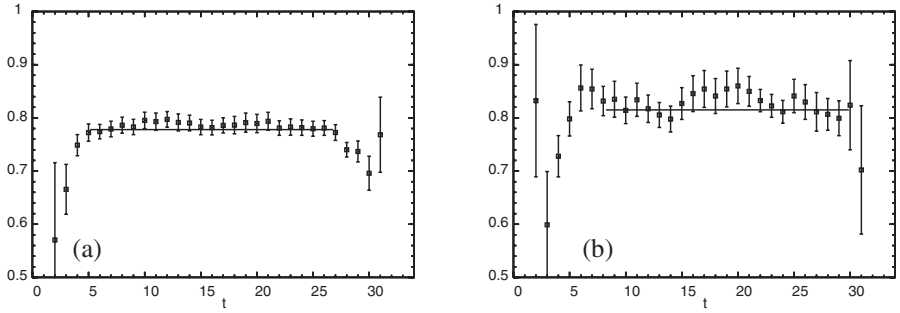

FIG. 3. Figure showing bare gauge invariant values of B_K as a function of the time slice corresponding to unquenched simulations with $m_{\rm sea} = 0.01/0.05$ (a) and $m_{\rm sea} = 0.02/0.05$ (b).

different values of the light sea quark masses. The parameters used in the unquenched simulations are collected in Table III. As in the quenched simulations we use degenerate quark kaons with the strange quark mass fixed to its physical value, so no extrapolation of the valence quark mass is necessary. A difference with the quenched analysis described in the last section is that for the unquenched case we only consider gauge invariant operators.

A first promising sign in our calculation is that there is little contamination from excited states, as can be seen in Fig. 3, where we have plotted the bare values of B_K as a function of the time slice. In particular, for $\beta = 6.76$, for which we have better statistics, we obtain an excellent plateau. To get the bare values of B_K given in Table IV, we perform fits to a constant over $5 \leq t \leq 27$ for $\beta = 6.76$ and over $8 \leq t \leq 30$ for $\beta = 6.79$. Results from the fits over the same ranges for the different four-fermion bare lattice operators involved in the calculation, normalized to the bare lattice value of the numerator in (8), are given in Table VII in the appendix.

The conversion of the values of the bare lattice operators to a value for $B_K^{\overline{MS}-NDR}(2\ \text{GeV})$ has been done perturbatively using the $\mathcal{O}(\alpha_s)$ lattice to continuum matching coefficients from [20] collected in the matrix (23). In the matching process it is most natural to take α_s in the V scheme with values for $N_f = 3$ from the recent 4-loops lattice determination in [47]—see Table III. The scale for α_s is not determined here so we consider various reasonable possibilities. One can also optimize the scale μ in Eq. (20) [48], but we have used $\mu = 1/a$ throughout this work.

TABLE IV. Values of the bare B_K and the one-loop renormalized $B_K^{\overline{MS}-NDR}(2\ \text{GeV})$ for the two values of the light sea quark masses and the corresponding statistical errors. The first number in the row labeled m_s is the mass of the degenerate up and down sea quarks and the second one is the mass of the strange sea quark.

$m_{\rm sea}$	$B_K^{\rm bare}$	$B_K^{\overline{MS}-NDR}(2\ \text{GeV})$
	$n_f = 2 + 1$ Asqtad	
0.01/0.05	0.785(11)	0.655(9)
0.02/0.05	0.815(18)	0.680(13)

The results we obtain for $B_K^{\overline{MS}-NDR}(2\ \text{GeV})$ performing the renormalization with $\alpha_V(1/a)$ are shown in Fig. 4. We plot the result as a function of the light sea quark mass and a decrease of the value of B_K with the reduction of the sea quark mass can be appreciated in this figure. For the degenerate valence quark case we are analyzing, the chiral behavior of B_K with the sea quark masses is linear, with the same coefficient for the strange, up and down sea masses [49]. We can thus extrapolate our results to the physical s and $u(d)$ masses, which yields the result

$$B_K^{\overline{MS}-NDR}(2\ \text{GeV}) = 0.618(18)(19)(30)(130). \qquad (25)$$

The first error in (25) is statistical, the second is from the extrapolation to the physical values of the sea quark masses, the third one is from discretizations errors and the final one is from the perturbative conversion to the $\overline{MS} - NDR$ scheme. The value in (25) is equivalent to

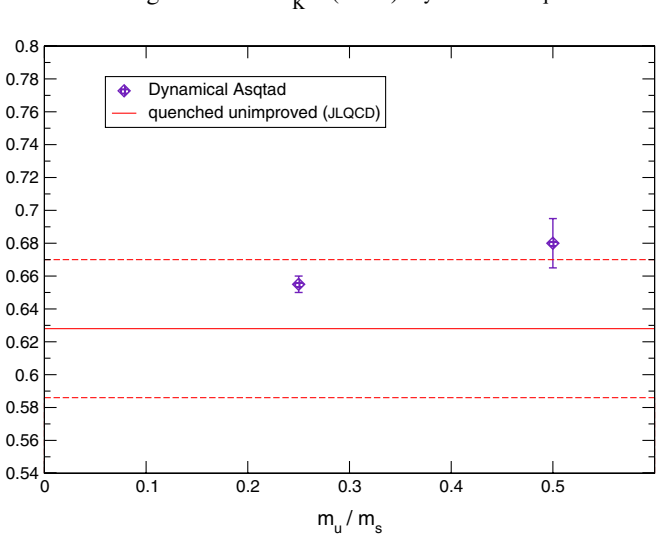

FIG. 4 (color online). Unquenched value of $B_K^{\overline{MS}-NDR}(2\ \text{GeV})$ as a function of the ratio between the light sea quark mass and the (real) strange quark mass. The lines represent the quenched results from [15]. Errors on the points are statistical only.

$\hat{B}_K = 0.83 \pm 0.18$, with $\hat{B}_K$ defined in (9). Note that this value of $\hat{B}_K$ is very similar to the previous quenched staggered result in [15] ($\hat{B}_K = 0.86 \pm 0.06$), so any final conclusion about the enhancement or decrease due to the inclusion of quark vacuum polarization effects in its calculation would need a significant reduction of the error quoted in (25).

If instead of using α_s in the V scheme to perform the renormalization at one-loop, we use α_S in the $\overline{MS}$ scheme at a scale $1/a$, the result we find is

$$B_K^{\overline{MS}-NDR}(2\text{ GeV}) = 0.637(19)(20)(31)(82). \quad (26)$$

This is the same as the result we obtain when using α_V with a scale close to $2/a$.

The total errors in (25) and (26) are dominated by the uncertainty associated with possible $\mathcal{O}(\alpha_s^2)$ corrections in the lattice to continuum matching process. On the finer MILC ensembles on which we are planning to redo our calculation as the next step in the improvement of the work presented here, the perturbative error bar would be reduced since the value of $\alpha_s(1/a)$ would be smaller. Using the existing MILC configurations with $a = 0.093$ fm, the perturbative error could be reduced from 20% to 14% (or from 14% to 9% if we use $\alpha_{\overline{MS}}(1/a)$ in the matching). In view of the improved scaling behavior we obtained in the quenched approximation within the Asqtad action described in Sec. IV, results for two lattice spacings will be enough to perform a reliable continuum extrapolation, reducing the discretization errors (third error in (25)). However, what is really needed to reduce the final error in (25) to a few percent level is a 2-loop matching or a nonperturbative matching method, that eliminates the uncertainty on the possible $\mathcal{O}(\alpha_s^2)$ corrections.

Discussion of the perturbative error

The naive error associated with the perturbative matching that we quote in (25) is just the result of multiplying our central value for $B_K^{\overline{MS}-NDR}(2\text{ GeV})$ by $(\alpha_V(1/a))^2$. In the same way, the perturbative error in (26) is the product of $B_K^{\overline{MS}-NDR}(2\text{ GeV})$ in that equation and $(\alpha_{\overline{MS}}(1/a))^2$. At the lattice spacing we are working, the unquenched values of α_V are large—see Table III- and translate into a $\sim$20% error in the result for $B_K^{\overline{MS}-NDR}(2\text{ GeV})$.

In principle, we do not expect two-loop corrections as large as 20%, since for the Asqtad action there are perturbative corrections for both numerator and denominator in (8) that tend to cancel at any order in the expansion. In fact, the shift in the value of B_K due to the one-loop renormalization is only 18%. Further evidence in favor of smaller $\mathcal{O}(\alpha_s^2)$ corrections is the fact that the difference between the results we obtain doing the matching with α_s at $q^* = 1/a$ and $q^* = 2/a$, that can be taken as an estimate of the uncertainty from the truncation of the perturbative series, is around 4%. The perturbative uncertainty estimated by squaring $\alpha_{\overline{MS}}(1/a)$, 13%, then seems more realistic. On the other hand, we believe that taking the two-loop error to be just the square of the one-loop shift [6] could be an underestimate of the error in the absence of other information.

VI. SUMMARY AND CONCLUSIONS

Most of the previous lattice calculations of B_K, in particular, those used in the UT analysis, were performed in the quenched approximation. This induces a large, essentially unknown and irreducible systematic error into the result. Precise simulations with sea quarks are necessary in order to be able to make full use of the experimental data on ε_K to constrain the CKM matrix. These unquenched simulations are feasible with present computers using staggered fermions at light sea quark masses. However, the unimproved staggered action suffers from large taste-changing interactions that generate important scaling corrections, as those found by the JLQCD collaboration. We have shown in Sec. IV that the scaling behavior is much better when using improved staggered actions.

This reduction of the discretization errors, together with the existence of unquenched configurations with relatively small sea quark masses, makes improved staggered actions an ideal choice for accurate calculations of B_K that incorporate light quark vacuum polarization effects. As a first step in this study we have calculated B_K with the Asqtad action in two ensembles at $a = 0.125$ fm and with two different light sea quark masses. In doing that, we have used the recent results for the one-loop matching coefficients in [20]. We obtain, using $\alpha_V(1/a)$,

$$B_K^{\overline{MS}-NDR}(2\text{ GeV}) = 0.618 \pm 0.136 \quad \text{or, equivalently,}$$
$$\hat{B}_K = 0.83 \pm 0.18, \quad (27)$$

or, performing the perturbative matching with $\alpha_{\overline{MS}}(1/a)$,

$$B_K^{\overline{MS}-NDR}(2\text{ GeV}) = 0.637 \pm 0.092 \quad \text{or, equivalently,}$$
$$\hat{B}_K = 0.85 \pm 0.12. \quad (28)$$

Both results are compatible within errors with other preliminary unquenched determinations [17,18,22–24].

The error needs to be reduced further. Some reduction can be achieved by working on finer lattices and incorporating staggered chiral perturbation theory results [49], but a large reduction will require matchings coefficients calculated beyond $\mathcal{O}(\alpha_s)$.

Another issues we would like to investigate in the future are the impact of SU(3) breaking effects and the chiral limit value of this quantity that could be compared to recent continuum calculations [10].

ACKNOWLEDGMENTS

This work was supported by European Commission (EC) Hadron Physics I3 Contract No. RII3-CT-2004-

506078 and Marie Curie Grant No. MEIF-CT-2003-501309, by PPARC, the US Department of Energy and the National Science Foundation. Calculations were done at NERSC. We thank the MILC collaboration for making their unquenched gauge configurations available. We thank UKQCD for their quenched configurations. We thank T. Becher and K. Melnikov for useful discussions about the renormalization of B_K.

APPENDIX: DETAILS OF CALCULATION RESULTS

In this appendix we collect the different four-fermion bare lattice matrix elements involved in the calculation of B_K for all the cases we analyze in this work.

TABLE V. Values of the gauge invariant and gauge noninvariant bare matrix elements in the quenched approximation, shown as a ratio with the denominator in (8) for unimproved staggered fermions.

β	$\sum A_i^{(1)}$	$A_4^{(1)}$	$\sum A_i^{(2)}$	$A_4^{(2)}$	$\sum V_i^{(1)}$	$V_4^{(1)}$	$\sum V_i^{(2)}$	$V_4^{(2)}$
Unimproved $n_f = 0$ (gauge invariant operators)								
5.70	0.026(1)	0.226(1)	0.012(1)	0.775(1)	−0.143(1)	−0.010(1)	−0.009(1)	−0.002(1)
5.93	0.217(5)	0.332(2)	0.091(2)	0.809(2)	−0.551(7)	−0.079(2)	−0.065(1)	−0.0182(4)
Unimproved $n_f = 0$ (gauge noninvariant operators)								
5.70	0.035(1)	0.276(1)	0.014(1)	0.772(1)	−0.176(1)	−0.013(1)	−0.010(1)	−0.002(1)
5.93	0.211(3)	0.346(1)	0.080(1)	0.800(2)	−0.571(5)	−0.077(1)	−0.056(1)	−0.015(1)

TABLE VI. Values of the gauge invariant and gauge noninvariant bare matrix elements in the quenched approximation, shown as a ratio with the denominator in (8) for HYP staggered fermions.

β	$\sum A_i^{(1)}$	$A_4^{(1)}$	$\sum A_i^{(2)}$	$A_4^{(2)}$	$\sum V_i^{(1)}$	$V_4^{(1)}$	$\sum V_i^{(2)}$	$V_4^{(2)}$
HYP $n_f = 0$ (gauge invariant operators)								
5.70	0.048(1)	0.262(1)	0.016(1)	0.772(1)	−0.285(2)	−0.0194(4)	−0.0079(3)	−0.0016(1)
5.93	0.181(8)	0.333(4)	0.065(6)	0.798(5)	−0.540(13)	−0.061(3)	−0.042(3)	−0.009(1)
HYP $n_f = 0$ (gauge noninvariant operators)								
5.70	0.041(1)	0.279(1)	0.014(1)	0.769(1)	−0.278(1)	−0.017(0)	−0.008(0)	−0.001(0)
5.93	0.164(8)	0.344(4)	0.053(5)	0.796(5)	−0.550(1)	−0.058(2)	−0.039(3)	−0.008(7)

TABLE VII. Values of the gauge invariant and gauge noninvariant bare matrix elements in the quenched approximation and with $n_f = 2 + 1$ sea flavors, shown as a ratio with the denominator in (8) for Asqtad staggered fermions.

β	$\sum A_i^{(1)}$	$A_4^{(1)}$	$\sum A_i^{(2)}$	$A_4^{(2)}$	$\sum V_i^{(1)}$	$V_4^{(1)}$	$\sum V_i^{(2)}$	$V_4^{(2)}$
Asqtad gauge invariant operators								
$n_f = 0$								
5.7	0.049(6)	0.285(1)	0.018(1)	0.781(1)	−0.278(1)	−0.020(1)	−0.016(1)	−0.004(1)
5.93	0.198(6)	0.351(3)	0.077(4)	0.808(4)	−0.596(11)	−0.074(2)	−0.053(2)	−0.012(1)
$n_f = 2 + 1$ $m_{\text{sea}} = 0.01/0.05$ $m_{\text{val}} = 0.02$								
6.76	0.248(6)	0.316(5)	0.076 (2)	0.885(16)	−0.605(11)	−0.093(2)	−0.035(1)	−0.0092(4)
$n_f = 2 + 1$ $m_{\text{sea}} = 0.02/0.05$ $m_{\text{val}} = 0.02$								
6.79	0.244(8)	0.323(8)	0.080(3)	0.940(26)	−0.630(17)	−0.096(2)	−0.036(1)	−0.0099(4)
Asqtad gauge noninvariant operators								
$n_f = 0$								
5.7	0.047(1)	0.284(0)	0.017(0)	0.777(1)	−0.267(1)	−0.018(0)	−0.011(0)	−0.002(0)
5.93	0.164(4)	0.338(2)	0.066(2)	0.797(3)	−0.548(7)	−0.061(2)	−0.041(2)	−0.009(4)

[1] C. T. H. Davies *et al.* (HPQCD Collaboration), Phys. Rev. Lett. **92**, 022001 (2004).

[2] A. J. Buras, M. E. Lautenbacher, and G. Ostermaier, Phys. Rev. D **50**, 3433 (1994).

[3] A. J. Buras, hep-ph/9806471; G. Buchalla, A. J. Buras, and M. E. Lautenbacher, Rev. Mod. Phys. **68**, 1125 (1996).

[4] D. Becirevic, Proceedings of QCD-02, Montpellier, France, 2002 (unpublished).

[5] J. Charles *et al.* (CKMfitter Group), Eur. Phys. J. C **41**, 1 (2005); M. Bona *et al.* (UTfit Collaboration), J. High Energy Phys. 07 (2005) 028.

[6] U. Nierste, hep-ph/0511125.

[7] Y. Nir, hep-ph/0510413.

[8] A. Pich and E. de Rafael, Phys. Lett. **158B**, 477 (1985); J. Prades, C. A. Domínguez, J. A. Peñarrocha, A. Pich, and E. de Rafael, Z. Phys. C **51**, 287 (1991).

[9] K. G. Chetyrkin *et al.*, Phys. Lett. **174B**, 104 (1986); R. Decker, Nucl. Phys. **B277**, 660 (1986); N. Bilić, B. Guberina, and C. A. Domínguez, Z. Phys. C **39**, 351 (1988); R. Decker, Nucl. Phys. B, Proc. Suppl. **7**, 180 (1989).

[10] J. Prades, J. Bijnens, and E. Gámiz, hep-ph/0501177; J. High Energy Phys. 03 (2006) 048; O. Catà and S. Peris, J. High Energy Phys. 03 (2003) 060; S. Peris and E. de Rafael, Phys. Lett. B **490**, 213 (2000).

[11] J. Bijnens and J. Prades, J. High Energy Phys. 01 (**2000**)002; Phys. Lett. B **342**, 331 (1995); Nucl. Phys. **B444**, 523 (1995).

[12] J. Bijnens, E. Gámiz, and J. Prades (work in progress).

[13] M. Jamin, S. Peris, and E. de Rafael (work in progress).

[14] M. Wingate, Nucl. Phys. B, Proc. Suppl. **140**, 68 (2005); S. Hashimoto, in *Proceedings of ICHEP 2004*, edited by H. Chen, D. Lu, W. Li, and C. Lu (World Scientific, Singapore, 2005), Vol I, p. 77; C. Dawson, PoS, LAT2005 (2005) 007.

[15] S. Aoki *et al.* (JLQCD Collaboration), Phys. Rev. Lett. **80**, 5271 (1998).

[16] S. R. Sharpe, Nucl. Phys. B, Proc. Suppl. **53**, 181 (1997).

[17] Y. Aoki *et al.*, Phys. Rev. D **72**, 114505 (2005).

[18] T. Bae, J. Kim, and W. Lee, PoS, LAT2005 (2005) 335.

[19] E. Gámiz, S. Collins, C. T. H. Davies, J. Shigemitsu, and M. Wingate (HPQCD Collaboration), Nucl. Phys. B, Proc. Suppl. **140**, 353 (2005).

[20] T. Becher, E. Gámiz, and K. Melnikov, Phys. Rev. D **72**, 074506 (2005).

[21] E. Gámiz, S. Collins, C. T. H. Davies, J. Shigemitsu, and M. Wingate (HPQCD Collaboration), PoS, LAT2005 (2005) 47; Nucl. Phys. B, Proc. Suppl. **153**, 114 (2006).

[22] J. M. Flynn, F. Mescia, and A. S. B. Tariq (UKQCD Collaboration), J. High Energy Phys. 11 (2004) 049.

[23] F. Mescia, V. Gimenez, V. Lubicz, G. Martinelli, S. Simula, and C. Tarantino, PoS, LAT2005 (2005) 365.

[24] S. Cohen, PoS, LAT2005 (2005) 346.

[25] J. Kim, T. Bae, and W. Lee, PoS, LAT2005 (2005) 338.

[26] E. Follana, A. Hart, and C. T. H. Davies (HPQCD Collaboration), Phys. Rev. Lett. **93**, 241601 (2004); K. Y. Wong and R. M. Woloshyn, Phys. Rev. D **71**, 094508 (2005); C. Bernard *et al.*, PoS, LAT2005 (2005) 114; C. Bernard, hep-lat/0603011; S. Durr, C. Hoelbling, and U. Wenger, Phys. Rev. D **70**, 094502 (2004).

[27] G. P. Lepage, Phys. Rev. D **59**, 074502 (1999).

[28] T. DeGrand, A. Hasenfratz, and T. G. Kovacs, Phys. Rev. D **67**, 054501 (2003).

[29] C. W. Bernard *et al.* (MILC Collaboration), Phys. Rev. D **61**, 111502 (2000).

[30] K. Orginos, D. Toussaint, and R. L. Sugar (MILC Collaboration), Phys. Rev. D **60**, 054503 (1999).

[31] A. Hasenfratz and F. Knechtli, Phys. Rev. D **64**, 034504 (2001).

[32] S. Naik, Nucl. Phys. **B316**, 238 (1989); G. P. Lepage, Phys. Rev. D **59**, 074502 (1999); K. Orginos, D. Toussaint, and R. L. Sugar (MILC Collaboration), Phys. Rev. D **60**, 054503 (1999).

[33] E. Gulez, J. Shigemitsu, and M. Wingate, Phys. Rev. D **69**, 074501 (2004).

[34] C. W. Bernard *et al.*, Phys. Rev. D **64**, 054506 (2001).

[35] M. Luscher and P. Weisz, Commun. Math. Phys. **97**, 19 (1985); Phys. Lett. **158B**, 250 (1985); M. G. Alford, W. Dimm, G. P. Lepage, G. Hockney, and P. B. Mackenzie, Phys. Lett. B **361**, 87 (1995).

[36] F. Gliozzi, Nucl. Phys. **B204**, 419 (1982); H. Kluberg-Stern, A. Morel, O. Napoly, and B. Petersson, Nucl. Phys. **B220**, 447 (1983); S. R. Sharpe and A. Patel, Nucl. Phys. **B417**, 307 (1994).

[37] S. R. Sharpe, A. Patel, R. Gupta, G. Guralnik, and G. W. Kilcup, Nucl. Phys. **B286**, 253 (1987).

[38] S. R. Sharpe, Nucl. Phys. B, Proc. Suppl. **7**, 255 (1989).

[39] N. Ishizuka and Y. Shizawa, Phys. Rev. D **49**, 3519 (1994).

[40] W. j. Lee and S. Sharpe, Phys. Rev. D **68**, 054510 (2003).

[41] W. j. Lee and S. R. Sharpe, Phys. Rev. D **66**, 114501 (2002).

[42] S. Aoki *et al.* (JLQCD Collaboration), Phys. Rev. Lett. **80**, 5271 (1998).

[43] W. Lee, T. Bhattacharya, G. T. Fleming, R. Gupta, G. Kilcup, and S. R. Sharpe, Phys. Rev. D **71**, 094501 (2005).

[44] W. j. Lee and S. R. Sharpe, Phys. Rev. D **60**, 114503 (1999); C. Aubin and C. Bernard, Phys. Rev. D **68**, 034014 (2003).

[45] C. Aubin *et al.*, Phys. Rev. D **70**, 094505 (2004).

[46] A. Gray, I. Allison, C. T. H. Davies, E. Gulez, G. P. Lepage, J. Shigemitsu, and M. Wingate, Phys. Rev. D **72**, 094507 (2005).

[47] Q. Mason *et al.* (HPQCD Collaboration), Phys. Rev. Lett. **95**, 052002 (2005).

[48] A. Kronfeld, G. P. Lepage, M. Nobes, and H. Trottier (work in progress).

[49] R. S. Van de Water and S. R. Sharpe, Phys. Rev. D **73**, 014003 (2006); PoS, LAT2005 (2005) 348.